JOC _Article_

Theoretical Study of Electroreductive Intramolecular Coupling of Nonconjugated Olefinic and Aromatic Ketones

Naoki Kise

Department of Biotechnology, Faculty of Engineering, Tottori University, Koyama, Tottori 680-8552, Japan

kise@bio.tottori-u.ac.jp

The electroreductive cyclization of hept-6-en-2-one, octa-7-en-2-one, and 5-phenylpentan-2-one was investigated by ab initio (UHF/6-311++G**) and density functional (UB3LYP/6-311++G**) calculation methods. The high regio- and stereoselectivities previously reported for olefinic ketones (exo-trans) and 5-arylpentan-2-ones (endo-trans) were reconfirmed. These experimental results well agree with the computational outcome for the transition states in the intramolecular coupling of ketyl radicals generated by one-electron transfer to the ketones.

Introduction

The intramolecular cross-coupling of radicals with other functional groups attracts much attention in synthetic organic chemistry, because it provides a useful tool to access five- and six-membered rings.[1] Especially, the intramolecular addition of alkyl radicals to olefins has been so far extensively utilized for the construction of these ring systems.[2,3] On the other hand, a number of studies on the intramolecular addition of ketyl radicals to olefins have been reported by means of various methods[4] after the pioneering work using electrochemical reduction by Shono and co-workers.[5] They have also disclosed that the electroreductive methodology was effective for the intramolecular coupling of ketyl radicals with acetylenes,[6] aromatic rings,[7] nitriles,[8] and _O_-methyl oximes.[9] Among them, the electroreductive intramolecular couplings of nonconjugated olefinic[5] and aromatic

SCHEME 1
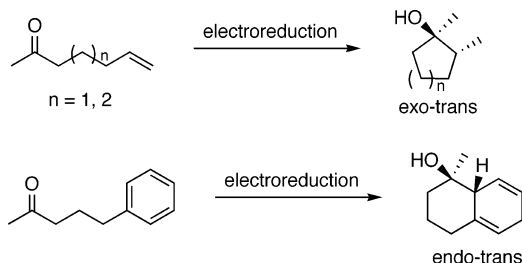
ketones[7] proceed regio- and stereoselectively to give trans isomers of five- or six-membered cyclized products predominantly (Scheme 1). In this paper, we calculated the energies of the intermediates and the transition states in these electroreductive cyclizations by ab initio and density functional methods to elucidate the high regio- and stereoselectives.

Results and Discussion

(1) Electroreductive Intramolecular Coupling of Hept-6-en-2-one. The electroreductive cyclization of hept-6-en-2-one was initially investigated (Scheme 2). Exo and endo cyclizations of ketyl radical **1** generated by one-electron transfer to hept-6-en-2-one produce five- and six-membered cyclized products **4** and **5**, respectively. It has been reported that the electroreduction of hept-6-en-2-one produced _trans_-**4** predominantly.[5] To verify the extremely high regio- and stereoselectivities, we reexamined this reaction using methanol−dioxane (1/1), ethanol, 2-propanol, or DMF as a solvent. It was confirmed that _trans_-**4** was the only product of the intramolecular coupling under the conditions in all the solvents employed, because _cis_-**4** and **5** could not be detected by ^{1}H NMR analysis of the products (endo/exo = trans/cis = >99/1).

(1) Giese, B. _Radicals in Organic Synthesis_: _Formation of Carbon−Carbon Bonds_; Pergamon Press: New York, 1986.

(2) For recent reports, see: (a) Jung, M. E.; Rayle, H. L. _J. Org. Chem._ **1997**, _62_, 4601. (b) Haney, B. P.; Curran, D. P. _J. Org. Chem._ **2000**, _65_, 2007. (c) Bennasar, M.-L.; Juan, C.; Bosch, J. _Chem. Commun._ **2000**, 2459. (d) Sun, Y.; Moeller, K. D. _Tetrahedron Lett._ **2002**, _43_, 7159. (e) Dhimane, A.-L.; Aissa, C.; Malacria, M. _Angew. Chem._, _Int. Ed._ **2002**, _41_, 3284.

(3) For recent theoretical studies on the radical cyclization, see: (a) Olivella, S.; Solé, A. _J. Am. Chem. Soc._ **2000**, _122_, 11416. (b) Leach, A. G.; Wang, R.; Wohlhieter, G. E.; Khan, S. I.; Jung, M. E.; Houk, K. N. _J. Am. Chem. Soc._ **2003**, _125_, 4271. For a review of theoretical and experimental studies on the radical addition to alkenes, see: (c) Fischer, H.; Radom, L. _Angew. Chem._, _Int. Ed._ **2001**, _40_, 1340.

(4) For recent reports using chemical reduction with SmI$_2$, see: (a) Molander, G. A.; McKie, J. A. _J. Org. Chem._ **1995**, _60_, 872. (b) Molander, G. A.; McWilliams, J. C.; Noll, B. C. _J. Am. Chem. Soc._ **1997**, _119_, 1265.

(5) (a) Shono, T.; Mitani, M. _J. Am. Chem. Soc._ **1971**, _93_, 5284. (b) Shono, T.; Nishiguchi, I.; Ohmizu, H.; Mitani, M. _J. Am. Chem. Soc._ **1978**, _100_, 545.

(6) Shono, T.; Nishiguchi, I.; Ohmizu, H. _Chem. Lett._ **1976**, 1233.

(7) (a) Shono, T.; Kise, N.; Suzumoto, T.; Morimoto, T. _J. Am. Chem. Soc._ **1986**, _108_, 4676. (b) Kise, N.; Suzumoto, T.; Shono, T. _J. Org. Chem._ **1994**, _59_, 1407.

(8) (a) Shono, T.; Kise, N. _Tetrahedron Lett._ **1990**, _31_, 1303. (b) Shono, T.; Kise, N.; Fujimoto, T.; Tominaga, N.; Morita, H. _J. Org. Chem._ **1992**, _57_, 7175.

(9) (a) Shono, T.; Kise, N.; Fujimoto, T. _Tetrahedron Lett._ **1991**, _32_, 525. (b) Shono, T.; Kise, N.; Fujimoto, T.; Yamanami, A.; Nomura, R. _J. Org. Chem._ **1994**, _59_, 1730.

SCHEME 2
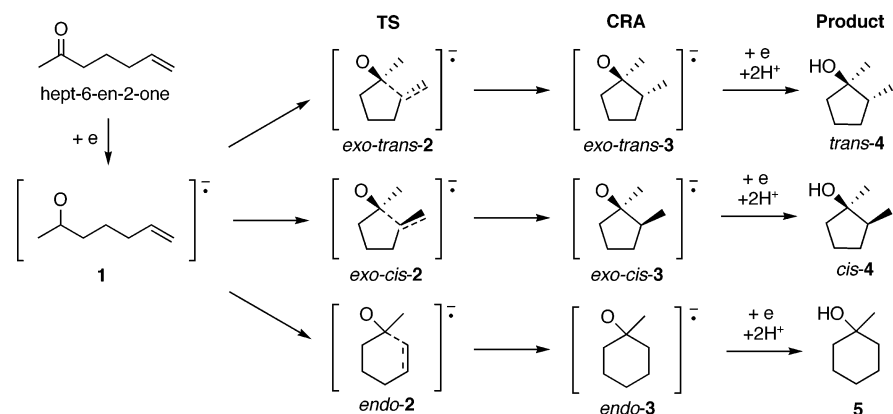
We carried out ab initio calculations at the UHF/6-311++G** level for the reactant radical anion **1**, transition states (TS) **2**, and cyclized radical anions (CRA) **3**. Four and two transition states were found for the 5-exo and the 6-endo cyclizations, respectively (Figure 1). The
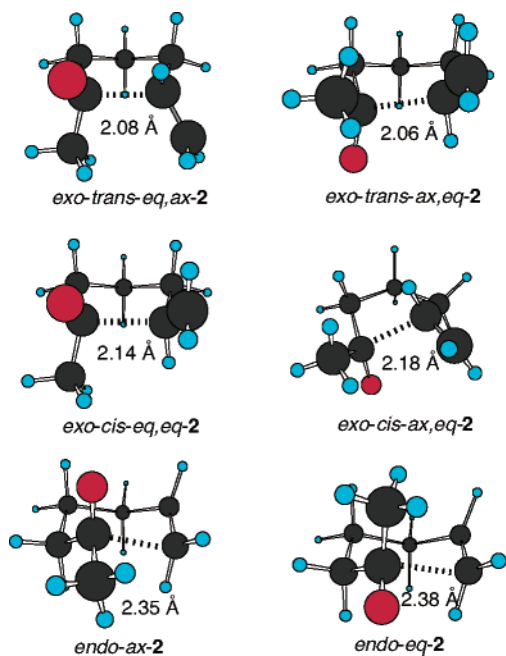

FIGURE 1. Transition states **2** for the cyclization of **1** optimized at the UHF/6-311++G* level.

energies of the six optimized structures for **2** and the corresponding **3** are given in Table 1 using the energy of **1** as reference. The trans/cis and exo/endo ratios were also calculated from the relative activation energies of the transition states according to the Maxwell–Boltzmann distribution law (Table 1).

First, it can be seen from Table 1 that the 5-exo cyclization is kinetically favored over the 6-endo cyclization, because the most stable transition state for the 5-exo cyclization (*exo-trans-ax,eq-***2**) is consistently more stable (4.3 kcal/mol in gas phase; 2.3 kcal/mol in ethanol) than those for the 6-endo cyclization (*endo-eq-***2**). In contrast, the 5-exo cyclized radical anions (*exo-***3**) are much higher in energy (at least 3.4 kcal/mol in the gas phase and 7.4 kcal/mol in ethanol) than the 6-endo cyclized radical anions (*endo-***3**). These results suggest that the high 5-exo

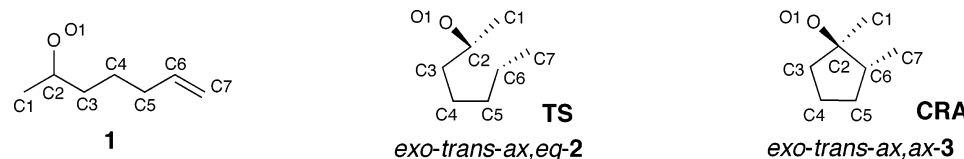**TABLE 1.   UHF/6-311++G**//UHF/6-311++G** Energetics of Cyclization of 1[a]**

	2 (TS)				**3** (CRA)	
	gas	PCM (EtOH)			gas	PCM (EtOH)
5-*exo-trans-eq,ax*	18.2	17.9 (9.3)		*eq,eq*	10.1	2.2
5-*exo-trans-ax,eq*	**16.1**	**16.3 (7.7)**		*ax,ax*	9.9	3.5
5-*exo-cis-eq,eq*	19.0	19.0 (10.1)		*eq,ax*	10.8	4.5
5-*exo-cis-ax,eq*	18.9	20.5 (10.6)		*ax,eq*	8.0	2.8
6-*endo-ax*	20.6	19.8 (10.8)		*ax*	*4.6*	−4.3
6-*endo-eq*	20.4	18.6 (9.9)		*eq*	6.0	−5.2
trans/cis	99/1	99/1 (98/2)				
exo/endo	>99/1	98/2 (98/2)				

[a] Energies are presented in kcal/mol with **1** as reference. The most stable transition states are in boldface and the most stable cyclized anion radicals are in italic. Trans/cis and exo/endo ratios are calculated from the relative activation energies of **2**. The values in parentheses are calculated by the UB3LYP/6-311++G**//UHF/6-311++G** method.

regioselectivity is determined not by thermodynamic control but by kinetic control. Such kinetic preference of the 5-exo cyclization and thermodynamic preference of the 6-endo cyclization were also reported for the cyclization of a 5-hexenyl radical.[3b] Next, the trans transition state (*exo-trans-ax,eq-***2**) is more stable than the cis transition state (*exo-cis-eq,eq-***2**) by as much as 2.7–2.9 kcal/mol (trans/cis = 99/1) for the exo cyclization. The computational results for the transition states, therefore, well agree with the experimental results of the electroreduction of **1**. Consequently, the most likely pathway for the high regio- and stereoselective cyclization of **1** is the kinetically controlled formation of *exo-trans-***3** from **1** through the most stable transition state *exo-trans-ax,eq-***2**.
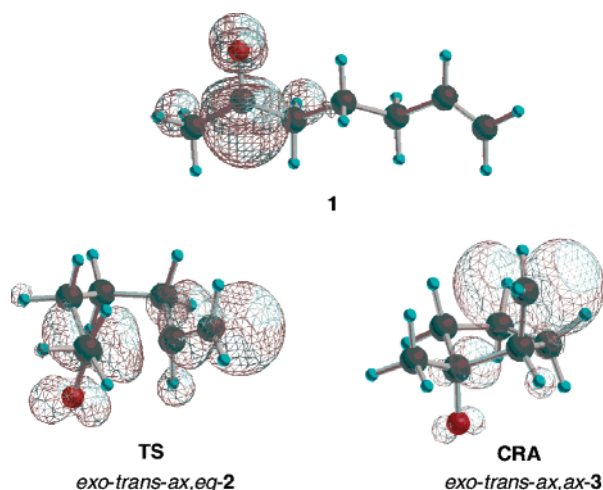
Charge and spin densities in **1**, *exo-trans-ax,eq-***2**, and *exo-trans-ax,ax-***3** calculated by the UHF/6-311++G** method are summarized in Table 2. In the previous report,[5] the trans stereoselectivity was explained by the electronic repulsion between the negatively charged C7 and O1 atoms. This intuitive explanation may not necessarily be right, because the C1 atom is also highly negative in *exo-trans-ax,eq-***2**. As illustrated in Figure 2, it can be appreciated that spin density is delocalized at the C2 atom in **1** and then moves to the C7 atom as the intramolecular coupling progresses.

(2) Electroreductive Intramolecular Coupling of Octa-7-en-2-one. Next, the electroreductive cyclization of octa-7-en-2-one was studied (Scheme 3). In this case,

TABLE 2.   Charge and Spin Densities of 1, *exo-trans-2*, and *exo-trans*-3 Calculated by the UHF/6-311++G** Method[a]

	1		*exo-trans-ax,eq-2*		*exo-trans-ax,eq-3*	
	charges[b]	spin densities	charges[b]	spin densities	charges[b]	spin densities
Cl	−0.04 (−0.07)	−0.33	−0.53 (−0.20)	−0.02	−0.40 (−0.08)	0.00
C2	−0.60	1.24	0.09	0.41	−0.06	0.09
C3	0.33 (0.26)	−0.43	−0.37 (0.18)	−0.07	−0.33 (−0.14)	−0.01
C4	−0.08 (0.02)	−0.06	0.11 (0.35)	−0.05	−0.42 (−0.23)	0.01
C5	−0.23 (−0.14)	−0.07	−0.77 (−0.60)	0.04	−0.67 (−0.42)	−0.01
C6	0.40(0.55)	0.01	0.57(0.78)	−0.54	0.93(l.14)	−0.30
C7	−0.59 (−0.42)	0.00	−0.86 (−0.71)	1.12	−0.78 (−0.59)	1.39
O1	−0.60	0.22	−0.53	0.15	−0.63	0.02

[a] Calculated by the Mulliken population analysis. [b] The values in parentheses are the atomic charges with hydrogens summed into heavy atoms.

FIGURE 2. Spin densities in **1**, *exo-tran-ax,eq*-**2**, and *exo-trans-ax,ax*-**3** calculated by the UHF/6-311++G** method (displayed by wire mesh).

it has also been reported that the exo-trans cyclization to give *trans*-**9** was exclusive.[5] The reexaminations of the electroreduction, however, disclosed that the formation of *trans*-**9** was not predominant (trans/cis = 88/12) contrary to the previous results,[5] although no seven-membered product **10** was obtained (exo/endo = >99/1).
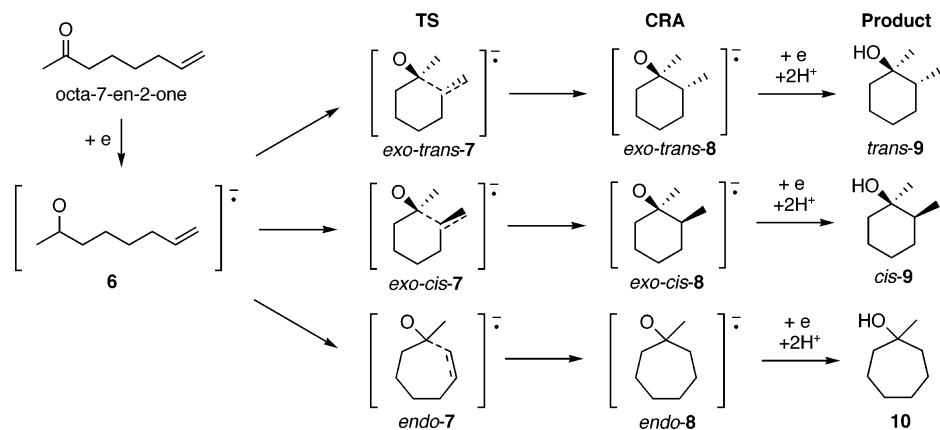
Calculations for the cyclization of ketyl radical **6** induced by one-electron transfer to octa-7-en-2-one gave four transition states for the 6-exo cyclization and two transition states for the 7-endo cyclization at both the UHF/6-311++G** (Figure 3) and the UB3LYP/6-311++G** levels (Figure 4). The energies of the optimized structures for the transition states **7** and the cyclized radical anions **8** are summarized in Table 3 together with the trans/cis and exo/endo ratios calculated from the relative activation energies. From the comparison of the activation energies, it is found that the exo-trans cyclization of **6** is kinetically preferred similarly to the cyclization of **1**. The differences in activation energies between the trans and cis transition states for the 6-exo cyclization seem to be evaluated to be somewhat low at the UHF/6-311++G** level (trans/cis = 84/16). The results of the calculations at the B3LYP/6-311++G** level with the PCM model, however, show excellent agreement with the experimental data (trans/cis = 88/12).

(3) Electroreductive Intramolecular Coupling of 5-Phenylpentan-2-one. Finally, the electroreductive cyclization of 5-phenylpentan-2-one was studied (Scheme 4). It was reconfirmed that the electroreduction of 5-phenylpentan-2-one gave trans six-membered cyclized product *trans*-**14** as the sole stereoisomer.[7] The formation of *cis*-**14** and five-membered cyclized product **15** could not be
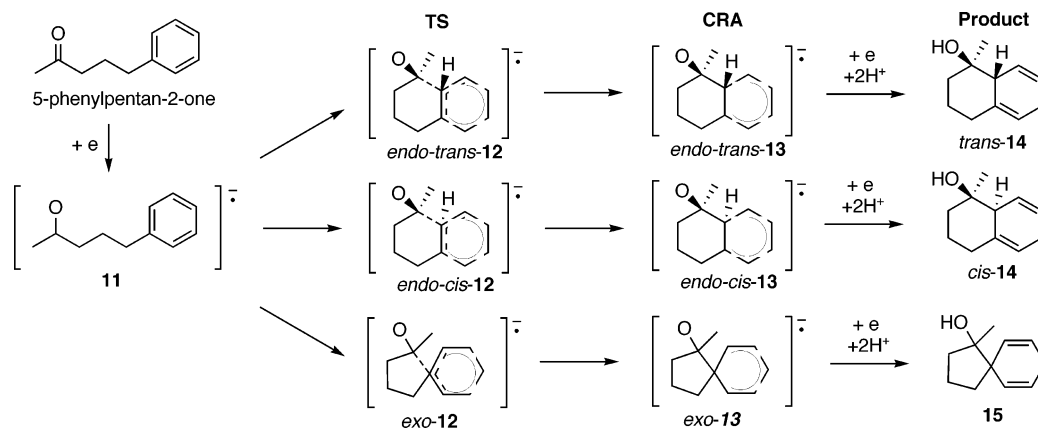
SCHEME 3

SCHEME 4

TABLE 3. **UHF/6−311++G**//UHF/6−311++G** and UB3LYP/6−311++G**//UB3LYP/6−311++G** Energetics of Cyclization of 6**[a]

| | UHF/6-311++G**//UHF/6-311++G** | | | | UB3LYP/6-311++G**//UB3LYP/6-311++G** | | | |
| | **7 (TS)** | | **8 (CRA)** | | **7 (TS)** | | **8 (C RA)** | |
	gas	PCM (EtOH)	gas	PCM (EtOH)	gas	PCM (EtOH)	gas	PCM (EtOH)
6-*exo-trans-eq,eq*	17.8	19.9 (10.2)	4.8	−0.7	17.8	1.8	17.5	−2.3
6-*exo-trans-ax,ax*	**14.6**	**18.9 (8.6)**	4.1	0.4	**13.7**	**0.5**	*13.7*	−2.2
6-*exo-cis-ax,eq*	15.6	19.9 (9.6)	*2.4*	−0.1	15.6	1.7	15.5	−0.9
6-*exo-cis-eq,ax*	20.1	22.0 (12.1)	5.9	0.7	20.2	4.0	18.9	−1.3
7-endo-ax	17.8	20.4 (10.6)	8.0	0.5	16.5	2.2	16.3	*−3.2*
7-endo-eq	20.4	21.4 (11.8)	8.9	0.2	18.7	3.1	18.5	−2.5
trans/cis	84/16	84/16 (84/16)			96/4	88/12		
exo/endo	>99/1	93/7 (97/3)			99/1	95/5		

[a] Energies are presented in kcal/mol with **6** as reference. The most stable transition states are in boldface and the most stable cyclized anion radicals are in italic. Trans/cis and exo/endo ratios are calculated from the relative activation energies of 7. The values in parentheses are calculated by the UB3LYP/6-311++G**//UHF/6-311++G** method.
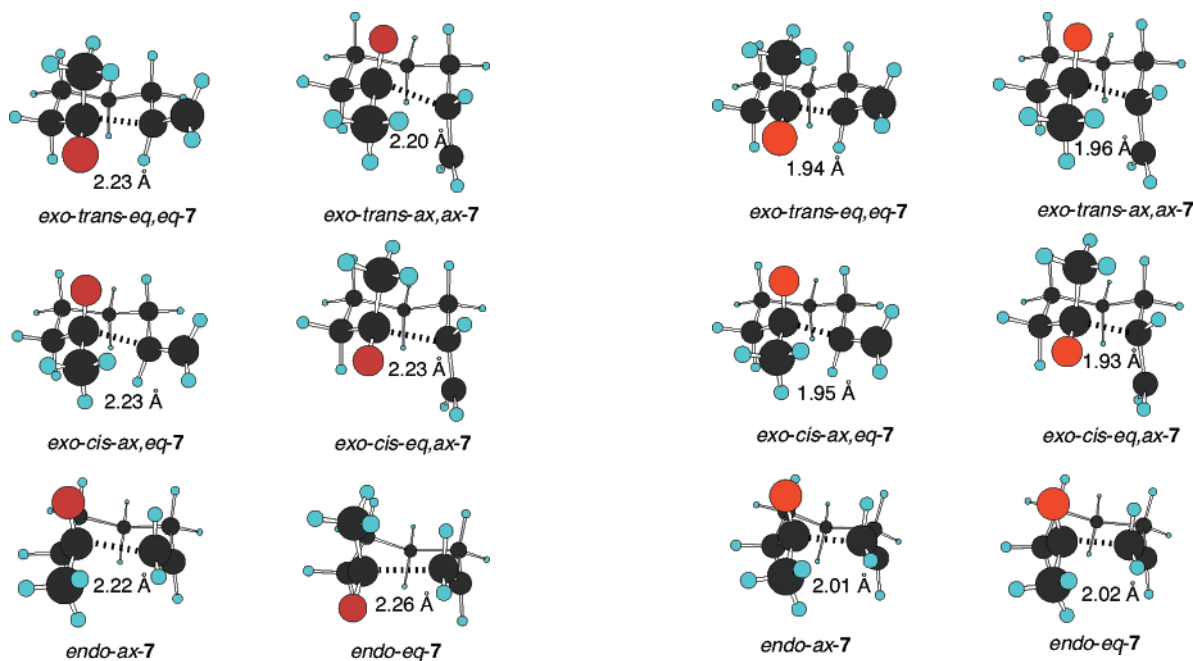

FIGURE 3. Transition states **7** for the cyclization of **6** optimized at the UHF/6-311++G** level.

FIGURE 4. Transition states **7** for the cyclization of **6** optimized at the UB3LYP/6-311++G** level.

detected by ¹H NMR analysis (endo/exo = trans/cis = >99/1). In our preliminary report,[7] the trans stereoconfiguration of predominantly formed **14** was assigned by transformation to its decahydro analogues. In this study,

we directly confirmed the stereostructure of *trans*-**14** by means of X-ray crystallographic analysis.

The results of the calculations for the cyclization of ketyl radical **11** generated by one-electron transfer to

TABLE 4. UHF/6-311++G**//UHF/6-311++G** Energetics of Cyclization of 11[a]

	12 (TS)		**13** (CRA)	
	gas	PCM (EtOH)	gas	PCM (EtOH)
6-*endo-trans*	**12.8**	**17.5 (9.8)**	*6.1*	*3.1*
6-*endo-cis*	14.7	20.0 (12.4)	8.1	6.1
5-*exo-ax*	15.5	21.7 (16.5)	11.7	13.1
5-*exo-eq*	20.2	24.7 (19.2)	17.2	15.1
trans/cis	97/3	99/1 (99/1)		
endo/exo	99/1	>99/1 (>99/1)		

[a] Energies are presented in kcal/mol with **11** as reference. The most stable transition states are in boldface and the most stable cyclized anion radicals are in italic. Trans/cis and exo/endo ratios are calculated from the relative activation energies of **12**. The values in parentheses are calculated by the UB3LYP/6-311++G**// UHF/6-311++G** method.
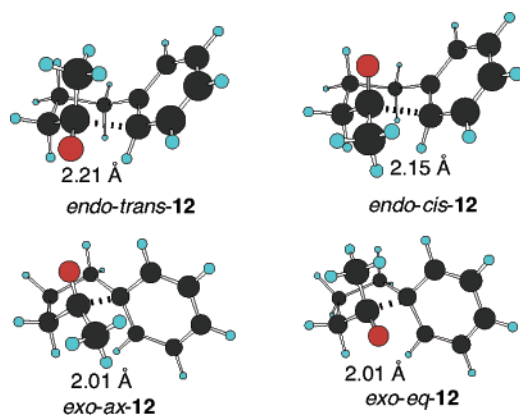
FIGURE 5. Transition states **12** for the cyclization of **11** optimized at the UHF/6-311++G** level.

5-phenylpentan-2-one are summarized in Table 4. Two transition states **12** were obtained for each of the 6-endo and the 5-exo cyclizations at the UHF/6-311++G** level (Figure 5). The results of the calculations show that the 5-exo cyclization giving spirocyclized product **15** can be disregarded, because the transition states for the 5-exo cyclization are much more unstable (>2.7 kcal/mol) than those for the 6-endo cyclization. The calculated relative activation energies of the trans and cis transition states for the 6-endo cyclization using the PCM method reveal good agreement with the exclusive formation of *trans-***14** in the experimental results (trans/cis = >99/1).

Spin densities in **11**, the most likely transition state *endo-trans-***12**, and the cyclized radical anion *endo-trans-***13** are listed in Table 5 and displayed in Figure 6. The spin density initially localized at the C2 atom in reactant **11** is delocalized to C6, C8, and C10 atoms in *endo-trans-***13**.

Conclusion

The intramolecular coupling of ketyl radicals generated by one-electron transfer to hept-6-en-2-one, octa-7-en-2-one, and 5-phenylpentan-2-one was computationally studied with ab initio and density functional methods to explain the high exo-trans and endo-trans selectivities observed in the electroreductive cyclization of olefinic ketones and aromatic ketones, respectively. The structures of the transition states and the corresponding cyclized radical anions were optimized for both exo and

TABLE 5. Spin Densities of 11, *endo-trans*-12, and *endo-trans*-13 Calculated by the UHF/6-311++G** Method[a]

	11	*endo-trans*-**12**	*endo-trans*-**13**
C1	−0.36	−0.08	0.05
C2	1.28	0.42	−0.05
C3	−0.52	−0.13	0.03
C4	0.02	0.01	−0.01
C5	−0.10	−0.07	−0.14
C6	0.04	0.67	1.00
C7	0.00	−0.69	−0.89
C8	0.00	0.80	1.02
C9	0.00	−0.65	−0.79
C10	−0.01	0.74	0.95
C11	0.01	−0.41	−0.28
O1	0.21	0.15	0.01

[a] Calculated by the Mulliken population analysis.
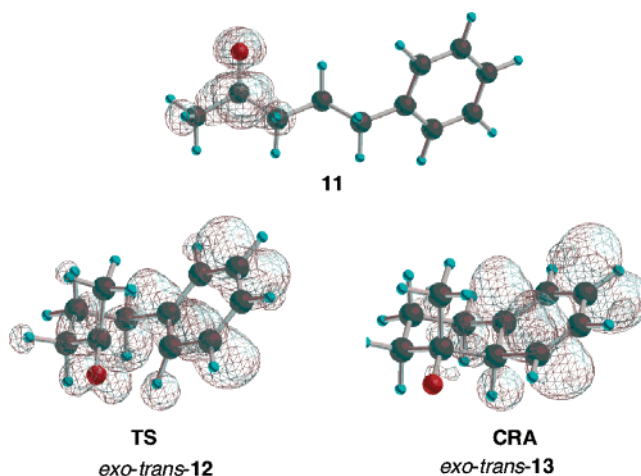
FIGURE 6. Spin densities in **11**, *exo-trans-***12**, and *exo-trans-***13** calculated by the UHF/6-311++G** method (displayed by wire mesh).

endo cyclizations of the ketyl radicals. Comparisons of the relative activation energies generally indicate good agreement with the high regio- and stereoselectivities in the experimental results. Therefore, it is concluded that the regio- and stereoselectivities in the cyclizations of the ketyl radicals are determined by kinetic control.

Experimental Section

Computational Methodology. All calculations were carried out with the Gaussian 98W program.[10] Geometry optimization was performed by the UHF/6-311++G** method throughout. Optimization with the UB3LYP/6-311++G** method succeeded only in the intramolecular coupling of octa-7-en-2-one. All optimized geometries were verified by the vibrational analysis and their energies were thermally corrected to 298 K based on the frequencies. As for the transition states, it was confirmed that these structures had only one imaginary frequency. The imaginary frequency was ascertained to be consistent with the intramolecular coupling by displaying the vibrational mode using the Gauss View program. In addition, single-point calculations were also carried

out for all optimized structures with the Tomasi solvent model (PCM) in EtOH at the same level as the geometry optimization (the UHF/6-311++G** or the UB3LYP/6-311++G* level) to take the solvent effect into consideration.

Typical Procedure for Electroreduction.[7] A solution of Et$_4$NOTs (5 g) in 2-propanol (20 mL) was put into a divided cell (40-mL beaker) equipped with an Sn cathode (5 × 5 cm^2),

a Pt anode (2 × 1 cm^2), and a ceramic cylindrical diaphragm (1.5-cm diameter). To the catholyte was added 5-phenylpentane-2-one (344 mg, 2 mmol). Electrolysis was carried out at a constant current of 0.1 A until almost all of the ketone was consumed (4 F∕mol). The catholyte was poured into water (50 mL) and extracted with Et$_2$O. The crude product was purified by column chromatography on silica gel (hexanes−ethyl acetates, 5/1) to give *trans*-**14** in 68% yield. Recrystallization of *trans*-**14** from hexanes−ethyl acetate (5/1) afforded single crystals for X-ray crystallographic analysis.

Supporting Information Available: X-ray crystallographic data (ortep) and NMR spectra of *trans*-**14** and the results of calculations for the transition states and the intermediates, as well as a crystallographic CIF file for *trans*-**14**. This material is available free of charge via the Internet at http://pubs.acs.org.

JO0356255

(10) Frisch, M. J.; Trucks, G. W.; Schlegel, H. B.; Scuseria, G. E.; Robb, M. A.; Cheeseman, J. R.; Zakrzewski, V. G.; Montgomery, J. A., Jr.; Stratmann, R. E.; Burant, J. C.; Dapprich, S.; Millam, J. M.; Daniels, A. D.; Kudin, K. N.; Strain, M. C.; Farkas, O.; Tomasi, J.; Barone, V.; Cossi, M.; Cammi, R.; Mennucci, B.; Pomelli, C.; Adamo, C.; Clifford, S.; Ochterski, J.; Petersson, G. A.; Ayala, P. Y.; Cui, Q.; Morokuma, K.; Malick, D. K.; Rabuck, A. D.; Raghavachari, K.; Foresman, J. B.; Cioslowski, J.; Ortiz, J. V.; Baboul, A. G.; Stefanov, B. B.; Liu, G.; Liashenko, A.; Piskorz, P.; Komaromi, I.; Gomperts, R.; Martin, R. L.; Fox, D. J.; Keith, T.; Al-Laham, M. A.; Peng, C. Y.; Nanayakkara, A.; Challacombe, M.; Gill, P. M. W.; Johnson, B.; Chen, W.; Wong, M. W.; Andres, J. L.; Gonzalez, C.; Head-Gordon, M.; Replogle, E. S.; Pople, J. A. *Gaussian 98W*, Revision A.9; Gaussian, Inc.: Pittsburgh, PA, 1998.